

Deep-Learning-Incorporated Augmented Reality Application for Engineering Lab Training

John Estrada^a, Sidike Paheding^b, Xiaoli Yang^a, Quamar Niyaz^a

^a*Department of Electrical and Computer Engineering, Purdue University
Northwest, 2200 169th Street Hammond, Hammond, 46323, IN, USA*

^b*Department of Applied Computing, Michigan Technological University, 1400 Townsend
Dr, Houghton, 49931, MI, USA*

Abstract

Deep learning (DL) algorithms have achieved significantly high performance in object detection tasks. At the same time, augmented reality (AR) techniques are transforming the ways that we work and connect with people. With the increasing popularity of online and hybrid learning, we propose a new framework for improving students' learning experiences with electrical engineering lab equipment by incorporating the abovementioned technologies. The DL powered automatic object detection component integrated into the AR application is designed to recognize equipment such as multimeter, oscilloscope, wave generator, and power supply. A deep neural network model, namely MobileNet-SSD v2, is implemented for equipment detection using TensorFlow's object detection API. When a piece of equipment is detected, the corresponding AR-based tutorial will be displayed on the screen. The mean average precision (mAP) of the developed equipment detection model is 81.4%, while the average recall of the model is 85.3%. Furthermore, to demonstrate practical application of the proposed framework, we develop a multimeter tutorial where virtual models are superimposed on real multimeters. The tutorial includes images and web links as well to help users learn more effectively. The Unity3D game engine is used as the primary development tool for this tutorial to integrate DL and AR frameworks and create immersive scenarios. The proposed framework can be a useful foundation for AR and machine-learning-based frameworks for industrial and educational

Email addresses: estradag@pnw.edu (John Estrada), spahedin@mtu.edu (Sidike Paheding), yangx@pnw.edu (Xiaoli Yang), qniyaz@pnw.edu (Quamar Niyaz)

training.

Keywords: artificial intelligence; augmented reality; machine learning; object detection; computer in education; lab equipment tutorial

1. Introduction

It is important for electrical engineers to understand how to use electrical equipment correctly. However, learning how to use equipment in a few cases has been a challenge for freshman electrical engineering students as many lab equipment are complex with several functionalities that are difficult to understand at the freshman level (Mejías Borrero and Andújar Márquez, 2012). Following lab or user manuals and watching video tutorials are traditional approaches to learn how to use equipment. However, they do not guarantee that students will retain all the information. With recent technological advancements, new teaching strategies that create immersive and hands-on experiences are being researched to increase students' interest and knowledge (Singh et al., 2019).

In this paper, we describe the design and development of a smartphone app that uses deep learning (DL) and augmented reality (AR) to create a learning platform for teaching students how to use electrical lab equipment. These new technologies with their integration into tools and applications used for day-to-day tasks have made life easier not only for students, but also for people in different roles. They also benefit manufacturing industries, gaming, education, health, farming, and a variety of other fields that require process automation (Ray, 2019). Artificial intelligence (AI) is used to complete complex tasks in the same way that humans do (Xue and Zhu, 2009). Extended reality (XR), a concept referring to virtual worlds and human-machine interactions, was developed to supplement the features that computers and mobile devices normally provide (Gong et al., 2021). Both AI and XR have the potential to be powerful workplace tools. For example, teams at various locations could work together in a virtual environment using AI and XR technologies to create new products and prototypes seamlessly. The applications of AI and XR are crossing many fields, ranging from workflow optimization in various healthcare processes and industrial training procedures to interactive educational systems (Nisiotis and Alboul, 2021). Augmented reality (AR) is one of the XR realities that is commonly used in mobile/tablet devices.

Deep learning (DL), a sub-field of machine learning (ML), embraces artificial neural networks (ANN), which are algorithms inspired by the structure and function of the human brain. ML has made significant advances in recent years because of the need for increased automation and intelligence (Khomh et al., 2018). XR refers to immersive technology that encompasses three distinct realities: AR, mixed reality (MR), and virtual reality (VR). AR superimposes three-dimensional objects on the physical world, requiring the use of mobile devices to create interactions. MR is a technology that combines the physical and digital worlds to create immersive physical experiences. Users interact with both the physical and digital worlds by using their five senses. VR is a fully digitized world in which users can completely immerse themselves in the computer-generated world by using virtual reality devices (Hu et al., 2020).

Many AR apps have recently been developed. AUREL (Ang and Lim, 2019) is an interactive application that aids in the understanding of specific STEM topics. It enhances the learning experience by projecting 3D models onto physical 2D textures that are part of the AR system, drawing virtual objects using the mobile display, and placing them onto a specific image tracked for the camera. The image detection for the ML system uses the camera as input data to detect specific images based on a trained dataset. Nonetheless, its application is limited to flat image recognition, allowing them to research and extend their idea for object recognition. An AR application (Thiwanka et al., 2018) was implemented to detect a breadboard and instruct students on how to build a circuit. Their system scans a circuit diagram for circuit symbols and their connections. These components are then arranged by a neural network. The AR system provides a 3D visualization of the scanned circuit diagram which students can use as a guided tutorial to build real circuitry. Another study (Sandoval Pérez et al., 2022) was to create and test an augmented reality application to teach power electronics to beginners. Two AR applications for RLC circuits and Buck–Boost converters were created, and the experimental results showed that they had a positive effect on students when compared to traditional teaching methods. The results of the experiment indicated improved cognitive performance. Despite the fact that augmented reality has made its way into STEM education, there is no general non-linear framework that can guide the development of an AR-based tutorial to our knowledge. Furthermore, the presented study goes in the direction of facilitating a smooth transition from real-time object recognition using deep learning methods to interactive tutorials using AR technologies,

a particular step of the process where there is potential for improvement.

In this paper, we discuss the design and implementation of an AR- and DL-based smartphone app to assist students in learning how to use electrical lab equipment such as multimeters. A similar framework can be applied to develop AR- and DL-based apps for other equipment in the future. The paper is structured as follows. Section 2 provides an overview of the DL and AR techniques suitable for this type of application. Section 3 illustrates the design and implementation of the smartphone app using different AR and DL frameworks. The experimental results are discussed in Section 4. Finally, the paper ends with a conclusion and future works in Section 5.

2. Overview of Deep Learning and Augmented Reality

This work explores the idea of using equipment recognition and an AR-based tutorial to enhance student learning experiences with electrical equipment in their engineering laboratories. Our long-term goal is to develop interactive smartphones apps for lab equipment such as multimeters, oscilloscopes, wave generators, and power supplies. Object detection using DL methods fits our goal because the app can detect specific electrical equipment in the lab with high precision in real-time using state-of-art DL algorithms. AR technology enables us to create virtual scenarios and integrate 3D models, animations, images, and videos embedded into teaching methods. In the developed app, the interactive visualization was created using the Unity3D game engine (Technologies, 2005). The object detection process of the app employs a deep neural network architecture trained with TensorFlow API (Yu et al., 2020).

2.1. Deep Learning

Innovative DL techniques for performing specific tasks have emerged rapidly in recent years due to significant advances in hardware development and data availability. For big data predictive analytics and multi-modal learning, DL algorithms are quite suitable, while traditional ML algorithms face several limitations. Studies in (Chen and Lin, 2014; Alom et al., 2019) point out that these DL methods are constructed with hierarchical layers and use complex neural networks to improve their performances iteratively. Machines equipped with DL models can perform specialized tasks such as driving a car, identifying weeds in a field, diagnosing diseases, evaluating machinery for errors, and even recognizing objects in real-time. They are

105 used in a wide range of computer science domains including computer vi-
106 sion (Alom et al., 2019), natural language processing (Deng and Liu, 2018),
107 and speech recognition (Deng et al., 2013). In this work, we are using a deep
108 neural network to detect objects. Object detection is primarily used in com-
109 puter vision and has gained popularity in a variety of applications over the
110 last decade, including autonomous vehicles, intelligent video, and surveillance
111 systems (Nishani and Çiço, 2017).

112 For object detection, a type of deep neural network called a convolu-
113 tional neural network (CNN) (LeCun et al., 1998) has been widely used.
114 CNN is a well-known DL algorithm that employs backpropagation in a feed-
115 forward neural network with a collection of neurons arranged in hierarchical
116 layers. It also exhibits typical neural network characteristics such as multi-
117 ple interconnected hidden layers (Pandiya et al., 2020; Arora et al., 2020).
118 CNN for object detection is trained on large labeled datasets and neural
119 network architectures that learn features directly from data without explicit
120 feature engineering. In recent years, object detection methods such as the
121 region-based convolutional neural network (RCNN) (Girshick et al., 2015),
122 you only look once (YOLO) (Redmon et al., 2016), and single shot detec-
123 tor (SSD) (Liu et al., 2016) have been proposed. The rapid development of
124 neural networks improves the accuracy and real-time performance of object
125 identification tasks significantly (Ryu and Kim, 2018). In this paper, we com-
126 pared RCNN and MobileNet-SSD v2 (Chiu et al., 2020) and observed that
127 MobileNet-SSD v2 has better performance for real-time applications in terms
128 of speed when implemented on mobile devices. It is important to note that
129 MobileNet-SSD v2 is a lightweight deep neural network architecture designed
130 specifically for mobile devices with high recognition accuracy. Therefore, we
131 employed MobileNet-SSD v2 in this work.

132 2.2. *Augmented Reality*

133 The relationship between the real and virtual worlds, as mentioned in
134 Section 1, is what distinguishes the various XR technologies. In AR, users
135 perceive virtual objects as real-world extensions, whereas MR users combine
136 and interact in both the real and digital world, and VR users immerse them-
137 selves entirely in a virtual world (Heirman et al., 2020; Andrade et al., 2020).
138 This paper focuses on the development of AR applications that allow us to
139 create experiences by utilizing additional digital data about our surround-
140 ings. We can receive digital information in real-time through devices such
141 as webcams, mobile phones, and tablets. In other words, AR allows us to

142 overlay layers of visual information in the physical world, allowing humans
143 to interact with virtual 3D objects as well as physical objects around us
144 (Dandachi et al., 2015). This feature has revolutionized the ways humans
145 learn and comprehend (Sendari et al., 2020). AR development necessitates
146 three key components: a physical object that serves as a model for the vir-
147 tual object’s interpretation and production; intelligence devices with access
148 to a camera that project an image of a targeted object; and software that
149 interprets the signal sent by the camera (Mahurkar, 2018).

150 There are diverse types of AR suitable for different applications despite
151 the fact that they all have similar capabilities (El Filali and Krit, 2019;
152 Poetker, 2018). Figure 1 depicts the two primary types of AR: marker-based
153 AR and marker-less AR.

154 2.2.1. *Marker-Based AR*

155 Marker-based AR works when it is triggered by pre-defined markers. It
156 allows the user to choose where to place the virtual object. Barcodes and QR
157 codes are commonly used as images or photo symbols to be placed on flat
158 surfaces. The program recognizes the marker when the mobile device focuses
159 the target image. The virtual information will be projected by the AR onto
160 the marker that will be displayed on the device. There are many levels
161 of complexity in marker-based AR (Gao et al., 2016). For example, a few
162 display virtual information when the device is focused on the marker, while
163 others save that virtual information and allow users to view it again when
164 the device is focused on a different section. The marker-based AR technology
165 leverages images from the actual world or QR codes to extract points, lines,
166 corners, textures, and other properties (Sendari et al., 2020). These images
167 are used to superimpose and create AR experiences by referencing track
168 points in the physical world.

169 2.2.2. *Marker-Less AR*

170 Marker-less AR is more versatile than marker-based AR. It interacts with
171 the real object without the need for pre-defined markers but leaves the free-
172 dom to the user. This allows the user, for example, to position a virtual object
173 anywhere on a real object. Users can experiment with different styles and
174 locations digitally without having to move anything in their immediate sur-
175 roundings (Vidya et al., 2014). Marker-less AR collects data from the device
176 hardware such as a camera, a GPS, a digital compass, and an accelerometer
177 for the AR program to function. Marker-less AR applications rely on com-

puter vision algorithms to distinguish objects, and they can function in the real world without specific markers (Beier et al., 2003; Pooja et al., 2020). There are four types of marker-less AR discussed as follows:

- (a) *Location-based AR*: In this type of AR, simultaneous localization and mapping (SLAM) technology is used to track the user’s location as the map is generated and updated on the user’s mobile device (Batuwanthudawa and Jayasena, 2020). To display AR content in the physical environment, the user must detect a surface with a mobile device (Unal et al., 2018; Argotti et al., 2002). As an example, the world-famous AR-based game app, Pokemon Go, uses SLAM technology that allows its users to battle, navigate, and search for 3D interactive objects based on their geographical locations (Ketchell et al., 2019).
- (b) *Superimposition-based AR*: Superimposition-based AR applications can provide an additional view along with the original view of the object. Object recognition is required to determine the type of object to partially or completely replace an object in the user’s environment with a digital image (Knopp et al., 2019; Soulami et al., 2019). Using HoloLens glasses, surgeons can superimpose images previously gathered through scanners or X-rays on the patient’s body during the operation. They can anticipate potential problems using this approach.
- (c) *Projection-based AR*: Projection-based AR (also known as projection mapping and augmented spatial reality) is a technique that does not require the use of head-mounted or hand-held devices. This method allows augmented information to be viewed immediately from a natural perspective. Using projection mapping, projection-based AR turns an uneven surface into a projection screen. This method allows for the creation of optical illusions (Lee et al., 2018).
- (d) *Outlining-based AR*: This type of AR employs image recognition to create contours or forms and highlight components of the real world using special cameras. It is used by human eyes to designate specific items with lines to make situations easier. Vuforia’s Model Target is an example of outlining-based AR. Vuforia is a platform that enables developers to quickly incorporate AR technology into their applications. Model Targets allow apps to recognize and track real-world objects based on their shape (Vuforia Developer Library, 2021).

In our project, we built a superimposition-based AR app. We built user interfaces on top of lab equipment, allowing step-by-step instructions to be

215 incorporated into the application for users to understand and learn how to use
216 specific equipment. Using AR technology, immersive experiences are created
217 in a variety of ways. It does, however, have some limitations such as the
218 inability to recognize multiple objects at once. On the other hand, DL models
219 show high performances in recognizing multiple objects at the same time.
220 Integrating AR apps with DL models will help trigger specific AR scenarios
221 based on objects being aimed at with a camera and allow an AR scenario to
222 perform a single tracking without decreasing mobile device performance.

223 **3. Design and Implementation of the AR App**

224 This section describes the design and development of the AR app that
225 integrates two independent frameworks for object detection and augmented
226 reality as shown in Figure 2. Unity 3D combines the output of these sys-
227 tems by inferring the object detection model with OpenCV and using an
228 AR dataset target with a Vuforia Engine. Furthermore, Unity 3D enables
229 the development of interactive user interfaces. Users can first use their mo-
230 bile device to infer the object detection model to detect the lab equipment.
231 The inference will classify and localize lab equipment that has been targeted
232 with the mobile camera. When an object is detected, a user interface (UI)
233 button appears, indicating that an AR-guided tutorial is available for the
234 object. Then, an AR scenario will be loaded, allowing students to use their
235 mobile camera to aim at a specific target. Following that, a 3D object will
236 superimpose on top of the physical object, activating UI panels with instruc-
237 tions on how to use the equipment.

238 The app development process consists of integrating a number of different
239 independent systems with their frameworks. In the interactive tutorial devel-
240 opment framework, Unity3D was used as the primary development software
241 for generating specific UI instructions and creating immersive interactions
242 between the mobile app and the user. The development framework was inte-
243 grated with a MobileNet-SSD DL model and a marker-less superimposition
244 AR that activates immersive modules containing 2D/3D objects. The de-
245 tailed framework integration is discussed below.

246 *3.1. Object Detection Framework*

247 MobileNet-SSDv2 (Chiu et al., 2020) architecture was used to build a
248 deep neural network model to detect electrical lab equipment. The archi-
249 tecture comprised MobileNet-v2 as the backbone network, an SSD detector,

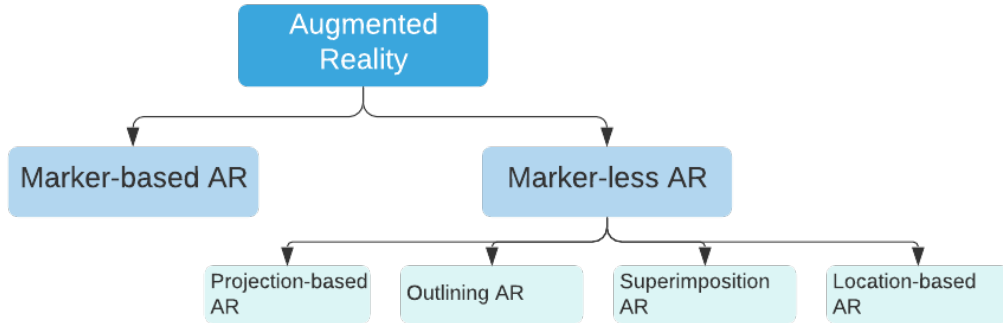


Figure 1: Types of augmented reality.

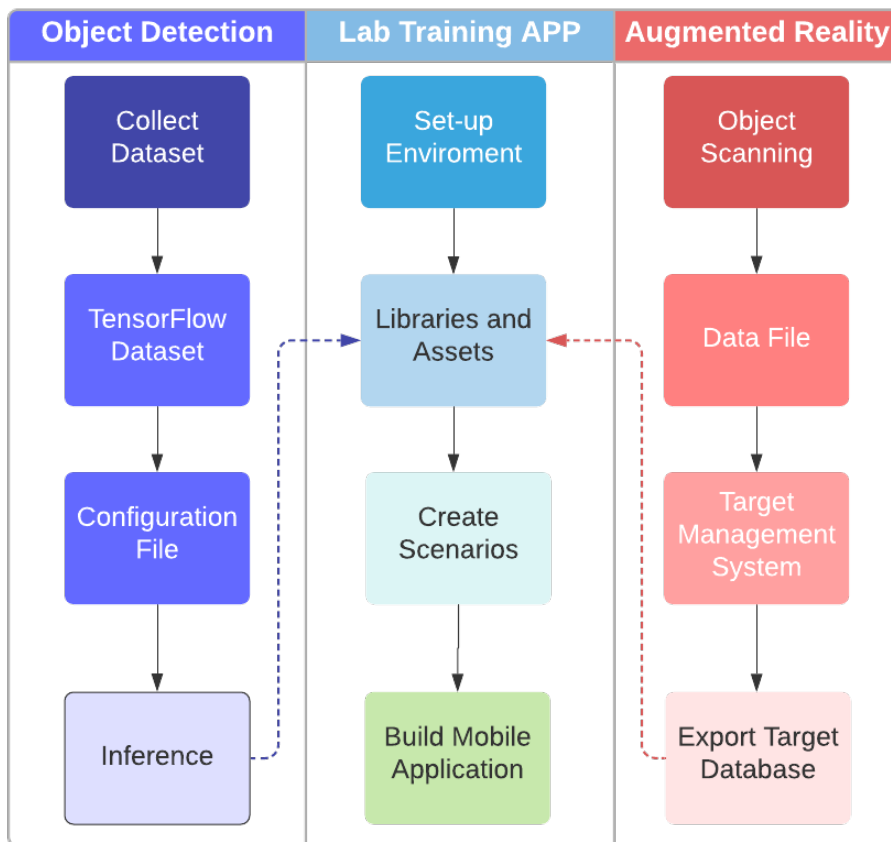


Figure 2: Design framework of AR-based smartphone app for lab equipment training.

and feature pyramid network (FPN). MobileNet, as the name implies, is intended for embedded applications on mobile devices to improve accuracy while effectively considering constrained resources. A loss function method was calculated using the predicted and labeled values of the classes and offsets to evaluate how the algorithm models the data. The confidence loss ($L_{confidence}$) occurs when attempting to predict a class, which is softmax loss over multiple classes confidences. Localization loss ($L_{localization}$) is defined as a mismatch between the ground truth and the intended boundary boxes (Liu et al., 2016; Zhang et al., 2020), where α is the weight coefficient, expressed as:

$$L_{loss} = L_{confidence} + \alpha \times L_{localization} \quad (1)$$

MobileNet is a low-latency and low-power model that can be tailored to meet the resource constraints of various use cases. For multi-scale object detection, MobileNetv2 provides a number of feature maps with different dimensions for the backbone detection network to the SSD convolutional layer that uses small convolutional filters to predict scores and class offsets for a fixed set of the standard bounding boxes. MobileNet-SSDv2 extracts features from images, which are then processed through SSD predictor layers that reduce image size to recognize objects at various scales (Chiu et al., 2020; Rios et al., 2021) as shown in Figure 3. Mobilenet-SSDv2 detector improves the SSD detector by combining MobileNetv2 and FPN while maintaining memory efficiency.

3.2. TensorFlow Object Detection API

TensorFlow (TF) API, developed by Google Brain, is a framework for creating a DL network (Yu et al., 2020). It is a powerful tool that can be used to create a robust object detection framework with a set of standard functions, eliminating the need for users to write code from scratch. It also provides a list of pre-trained models, which are useful not only for inference but also for building models with new data. Model Zoo is a collection of models that have been previously trained using the common objects in context (COCO) dataset (Phadnis et al., 2018). A workflow for training a DL model using the TF API is shown in Figure 4 and can be described through the following steps:

- (a) *Image Dataset*: The model was given input of 643 images collected from various perspective views and in different lighting settings. Each image is of 4032×3024 pixels in size. It is necessary to annotate these

images before using them to train the model. A software, `LabelImg` (Tzutalin, 2015), is used in the annotation process that allows users to draw a rectangle in a specific area of the image. During training, the annotation will help the model precisely locate the object in the image. The outlining will generate and save coordinate points in an XML file.

(b) *TensorFlow Dataset*: To make the computation of the DL framework efficient, TF records use a binary file format. Furthermore, TF records enable the dataset to be stored as a sequence of binary strings that improves the model’s performance while using less disk space. We converted the XML files generated by `LabelImg` into TF binary records using a Python script. The last step in configuring the TF dataset is to create a `.pbtxt` file containing all of the categorical label classes that will be stored in a TF record file.

(c) *Configuration File*: Multiple pre-trained models based on the common objects in context (COCO) dataset are available in TF. These models can be used to set up DL models prior to training on a new dataset. Table 1 lists several popular architectures with pre-trained models. For instance, `ssd_MobileNet_v1_coco` is the SSD with a MobileNet v1 configuration, `ssd_inception_v2_coco` represents an SSD with an Inception v2 configuration, and `faster_rcnn_resnet101_coco` stands for Faster R-CNN with a Resnet-101 (v1) configuration. All these configurations have been derived for the COCO dataset. From Table 1, it can be observed that `ssd_MobileNet_v1_coco` reaches the fastest inference speed of 30 ms but with the lowest mean average precision (mAP). In contrast, `faster_rcnn_resnet101_coco` has the slowest inference speed but the highest mAP of 32.

We tested both MobileNet SSD v2 and faster RCNN (Ren et al., 2015) and concluded that MobileNet SSD v2 performs faster inference in mobile devices than the faster-RCNN model in our study. Using a pre-trained model saves time and computing resources. A configuration file, in addition to the pre-trained model, is also required. It must match the same architecture of the pre-trained model. It is recommended to fine-tune the model to maximize the prediction outcome. The process of fine-tuning is divided into two steps: restoring weights and updating weights. After we completed the requirements, we ran the python code provided for TF API to start the training job. Following training, the API will generate a file serving as a training checkpoint in a specific

324 format named `.ckpt`. This file is a binary file containing all of the
325 weights, biases, and other variables' values.
326 (d) *Inference*: After training the model, the last step is to put it into
327 production and feed the model with live data to calculate the predicted
328 output. Before testing, we can evaluate the model's accuracy using
329 mAP. In Section 4, the evaluation result is described in detail. We also
330 need a lightweight version of the model to perform inference, so we
331 choose an OpenCV library.

332 In addition, there is a frozen trained model, a ready-to-use inference
333 model that can generate an output based on the live data input, and the
334 frozen process file is stored in Protobuf (`.pb`) file. The Protobuf model con-
335 tains graph definition and trained parameters in a binary format. The text
336 graph representation of the frozen process file is in a human-readable format
337 required by the OpenCV library and is kept in a `.pbtxt` format. After creat-
338 ing the corresponding file, it is time to examine and test the trained model.
339 We use a function called `VideoCapture` from OpenCV to test the model,
340 which loads the input video using the PC webcam and then predicts the
341 relevant labels and object location with an enclosed rectangle indicating its
342 pixel location within the input image. Finally, with the Protobuf and the
343 configuration file, we can now use the Unity3D game engine and OpenCV to
344 create our application by triggering AR scenarios based on the detection of
345 electrical lab equipment performed by the DL model during its inference.

346 3.3. *Augmented Reality Framework*

347 Vuforia is a framework that enables the creation, recognition, and tracking
348 of virtual and physical objects in the real world using an electronic device.
349 To test the prototype of our tutorial that integrates both object recognition
350 and interactive augmented reality, we developed a tutorial on how to use a
351 multimeter in the lab. A scene (a live video) captured by the camera will be
352 saved to a mobile device. The Vuforia SDK creates a frame (a single image
353 within a series of photos) of the captured scene. It improves the quality
354 of the image captured by the camera so that an AR tracker component
355 can correctly treat it. It uses the latter to analyze the image and search
356 the database for matches, which may include one or more targets. Finally,
357 the program renders virtual material such as photographs, videos, models,
358 and animations on the device screen, creating a hybrid image of what we
359 perceive as holographs. The process of generating AR targets is depicted in
360 Figure 5 and can be described in the following steps:

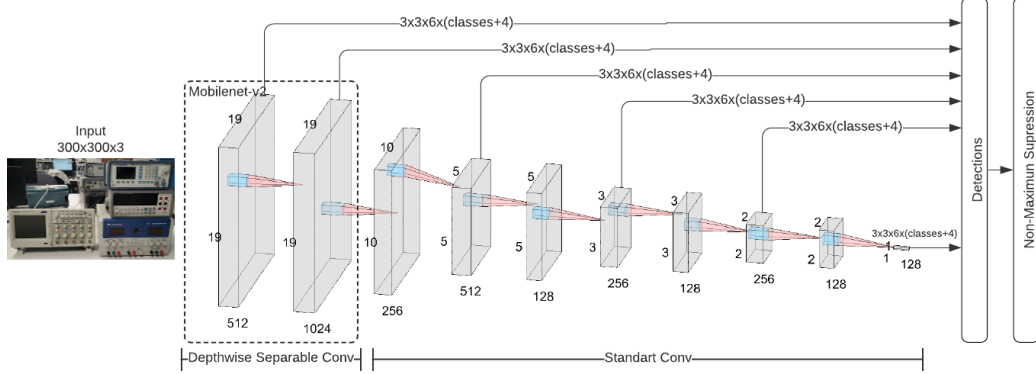


Figure 3: MobileNet SSD deep neural network architecture.

Table 1: Comparison Pre-Trained Model Zoo based on COCO Dataset Yu et al. (2020). *ssd_MobileNet.v1_coco* and *ssd_MobileNet.v2_coco* are the SSD with MobileNet v1 and v2 configurations, respectively. *ssd_inception.v2_coco* represents SSD with Inception v2 configuration, and *faster_rcnn_resnet101_coco* stands for Faster R-CNN with Resnet-101 (v1) configuration. All these configurations are for the COCO dataset.

Model name	Speed (ms)	COCO (mAP)	Output
<i>ssd_mobilenet.v1_coco</i>	30	21	Boxes
<i>ssd_mobilenet.v2_coco</i>	31	22	Boxes
<i>ssd_inception.v2_coco</i>	42	24	Boxes
<i>faster_rcnn_resnet101_coco</i>	106	32	Boxes

Note: Speed (ms) relates to the network’s inference speed, or how long it takes to produce an output based on the input. The mAP calculates a score by comparing the ground-truth bounding box to the detected box. The higher the score, the better the model’s detection accuracy is.

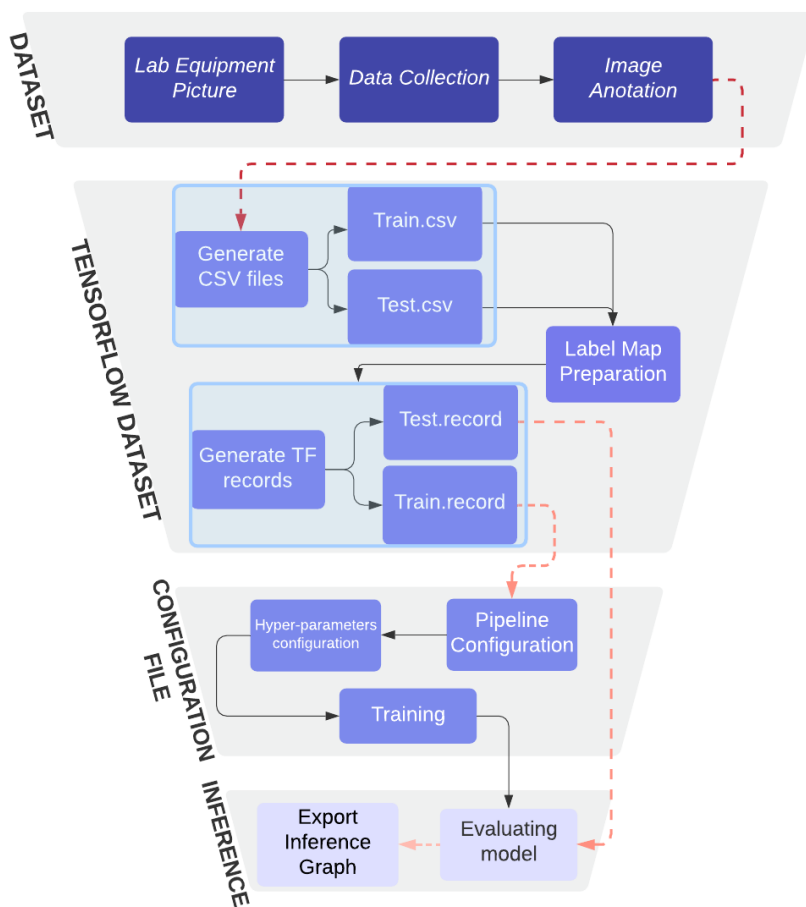


Figure 4: Object detection workflow using TensorFlow API.

- 361 (a) *Object Scanning*: It is the primary tool for generating an object data
362 file, which is required for generating an object target in the target
363 manager on the Vuforia webpage. This app is available on the Vuforia
364 developer website, which users can access after creating a developer ac-
365 count. The ObjectScanner (Park and Chin, 2019) app is used, and the
366 scanning environment is configured. The Vuforia developer portal pro-
367 vides a printable target image that defines the target position and ori-
368 entation relative to the local coordinate space to scan the object and
369 collect data points. It also distinguishes and removes undesirable areas.
370 This printable target image is used in conjunction with an Android ap-
371 plication, which is available for free download from the Vuforia official
372 website. During scanning, the printable target image must be placed
373 under the object to be scanned. Using the Vuforia scanning mobile
374 application, the user can start collecting data points from the object.
375 To achieve the best scanning quality, it is recommended to work in a
376 noise-free environment with moderately bright and diffuse lighting. It
377 is also recommended to avoid objects with reflective surfaces. In this
378 work, a multimeter met all of the requirements, and a successful scan-
379 ning was achieved.
- 380 (b) *Data File*: Following the scanning, an object data file is created. The mo-
381 bile app will also show how many scanning points the object has.
382 The completed scanning area is evidenced by a square grid that changes
383 color from gray to green. The object data file contains all the object’s
384 information. There is a test scenario to determine whether the scanned
385 object has sufficient data for augmentation. In this scenario, a green
386 rectangular prism will be drawn in one of the object corners relative to
387 the target image coordinate space.
- 388 (c) *Target Management System*: Vuforia has a framework that allows de-
389 velopers to choose from various target types, such as picture targets,
390 stimuli targets, cylinder targets, object targets, and VuMarks. The sys-
391 tem will process and manage the data for visual examination. A devel-
392 oper license is required to fully utilize the Vuforia manager web-based
393 tool, which includes access to a target manager panel where a database
394 can be uploaded, and targets can be added to the management system.
395 The 3D object option must be selected when selecting the target type,
396 and the object data file must be uploaded.
- 397 (d) *Export Target Dataset* Following the web-tool processing the informa-
398 tion, the database can be downloaded by choosing the desired platform.

The platform can be converted into a package that can be used in the primary development process as well as to create AR experiences in Unity.

3.4. Lab Training Application Framework

With the help of AR and DL, the equipment learning application focuses on teaching and improving the student's learning experience on how to properly use electrical equipment. Unity3D will provide libraries that allow these technologies to be combined on top of assets, animations, and 3D models to create training scenarios that will engage students in learning through experience. The development procedure is shown in Figure 6 and can be described in the following steps:

- (a) *Setup Environment*: The setup starts with the creation of a new project using a Unity hub. After creating and opening the project, it is essential to switch to a different build platform because Unity allows us to create once and deploy anywhere. In other words, we can select a platform from the list of available platforms in Unity, such as Windows, WebGL, Android, iOS, or any gaming console. We chose Android as the deployed platform for this project. The platform can be changed in the build settings windows, which can be accessed via the file bar. Additionally, the rendering, scripting, and project configuration must be modified.
- (b) *Libraries and Assets*:
 - (1) OpenCV Library: OpenCV For Unity (Enoxsoftware, 2016) is a program that uses AI algorithms to analyze and interpret images on computers or mobile devices. This Unity asset store product allows users to test AI pre-trained models that can be used to run algorithms and executable applications on mobile devices. The model employs a script that requires a binary file of a DL model with trained weights (weights of deep neural networks are not modified in this stage), and a file model network configuration. This script is granted access to the device resource, specifically the camera, so that the script can pass input to the model and start object detection inference, which will generate bounding boxes and labels around the object detected.

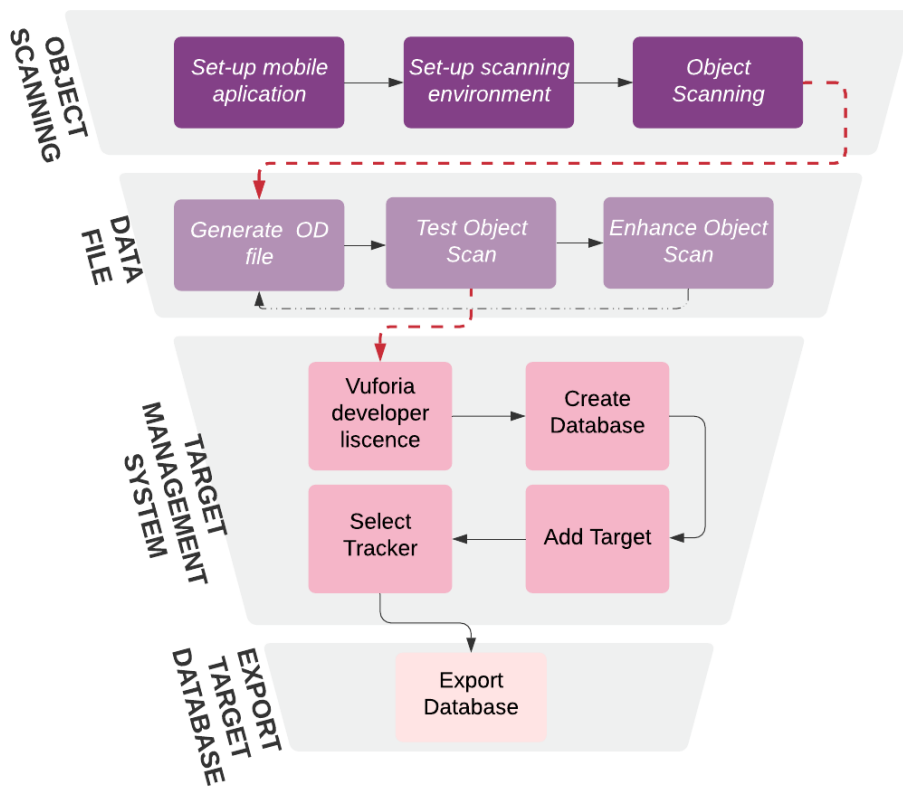


Figure 5: Vuforia object tracking framework.

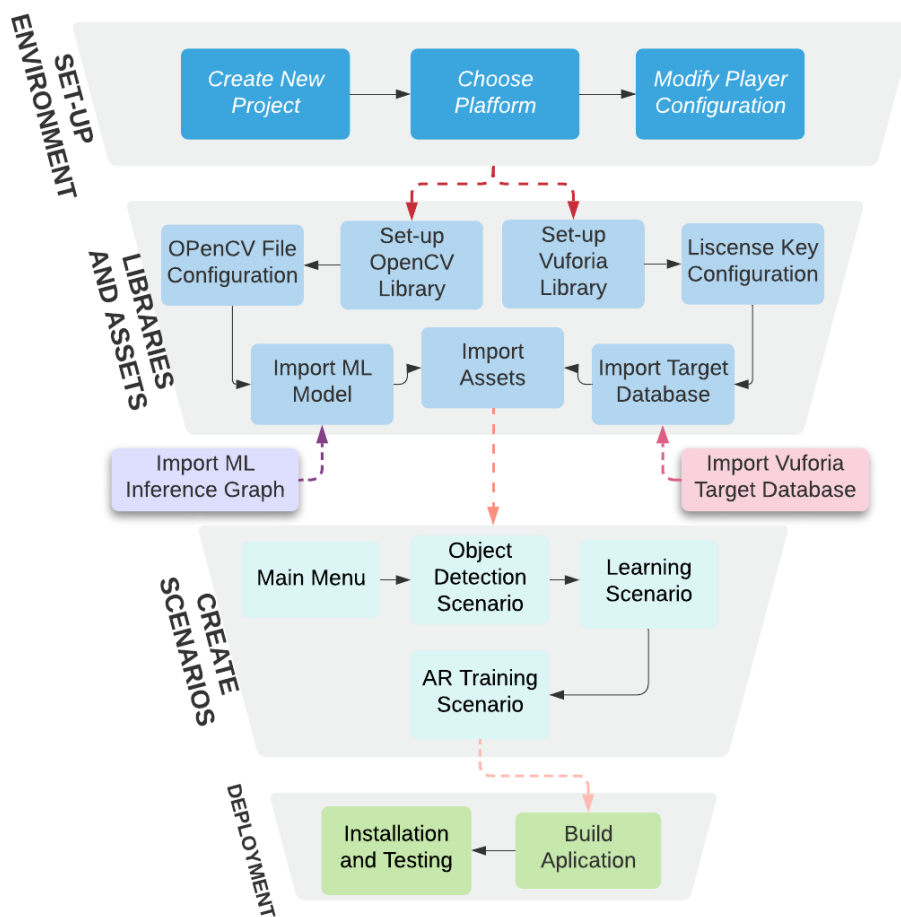


Figure 6: Lab training application framework.

- 433 (2) Vuforia Engine: This library allows Unity to create AR experi-
 434 ences for mobile devices. It is a collection of scripts and pre-made
 435 components for developing Vuforia apps in Unity. It includes API
 436 libraries written in the C# language that expose the Vuforia APIs.
 437 This library supports all traceable functions as well as high-level
 438 access to device hardware such as the device camera.
- 439 (3) Assets: They are graphical representations of any items that could
 440 be used in the project. It is made up of user interface sprites, 3D
 441 models, images, materials, and sounds, all with their own design
 442 and functionality. Photoshop is used to create art sprites, such as
 443 images for a virtual manual and blender. A 3D modeler software
 444 is used to create 3D models.
- 445 (c) *Scenarios creation*
- 446 (1) Main menu: The application includes a menu scenario, as shown in
 447 Figure 7, that will allow the user to select various modes based on
 448 their preferences. It includes a tutorial that teaches students how
 449 to use the application. There is a training mode to help students
 450 learn more about lab equipment or electrical components.
- 451 (2) Object detection: In this case, the DL model is used in conjunc-
 452 tion with the OpenCV library in Unity. The application has access
 453 to the device’s camera from which it will infer the object detection
 454 model provided by the object detection framework. Furthermore,
 455 depending on the object that is being targeted, the application au-
 456 tomatically generates bounding boxes around the desired object
 457 with its respective label and confidence. When the user points to
 458 the desired equipment, a bottom panel will appear with the option
 459 to load the AR experience or continue looking for other lab equip-
 460 ment. The OpenCV library allows us to specify the desired confi-
 461 dence value threshold during the model inference. During model
 462 inference, we can specify the desired confidence value threshold
 463 using the OpenCV library. The model draws a green rectangle
 464 around the detected equipment. The detection threshold confi-
 465 dence value is set to 90%, which means that the confidence must
 466 be greater than or equal to 90% to indicate a detection with a rect-
 467 angular bounding box. This percentage was chosen because the
 468 lab equipment is quite different. The score of 90% would ensure
 469 that the lab equipment detected had a high confidence level.
- 470 (3) Learning scenarios: A 3D visual aid is provided in this scenario to

471 understand the essential functions of the equipment selected dur-
472 ing the detection scenario. Figure 8 shows how users will be able
473 to access an interactive 3D model representation of the equipment
474 or view the equipment from various perspectives. In other words,
475 it is a virtual manual introductory guide.

476 (4) AR training scenario: When the application detects an object
477 that has previously been configured in Unity, a 3D model will be
478 superimposed on top of the physical object in the mobile app.
479 It will also include a UI for the user to interact with, allowing
480 them to understand and explore the physical object, while the
481 mobile application provides additional information in the form of
482 holograms, as shown in Figure 9.

483 (d) *Deployment*: The final step of the framework is to build the project for
484 the desired end platform, which can be Android or iPhone. The sce-
485 narios in Unity must be selected and linked together. Unity will launch
486 and generate a platform associated file that can be directly installed
487 on mobile devices.

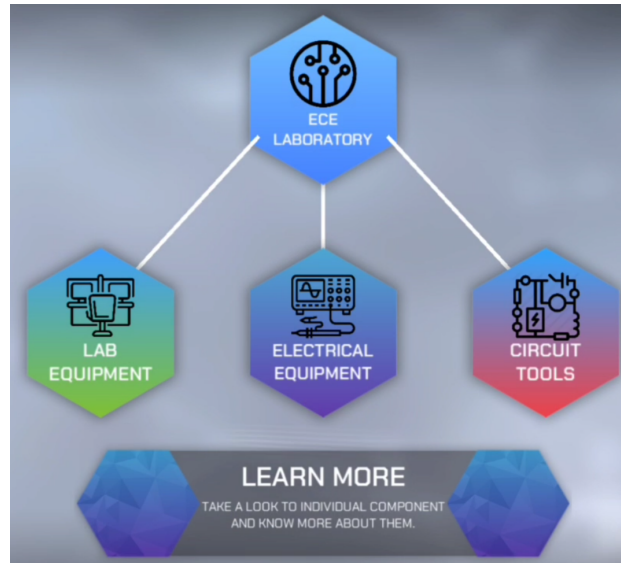


Figure 7: Main menu interface.

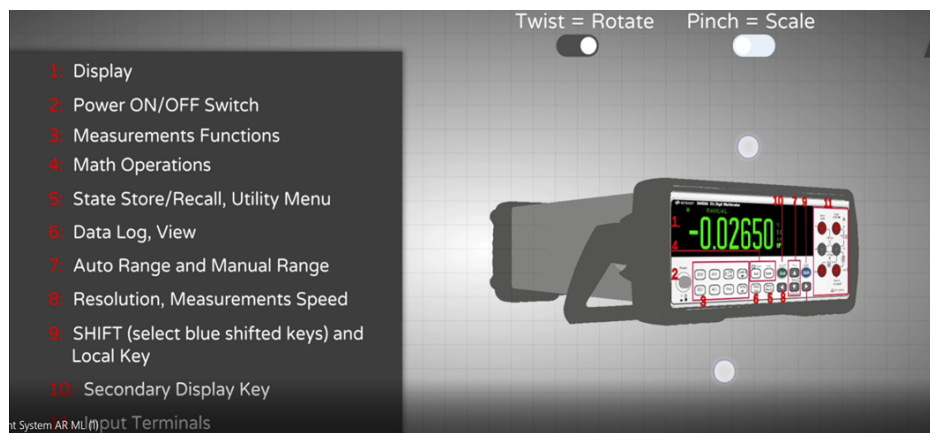


Figure 8: Learning interactive scenario.

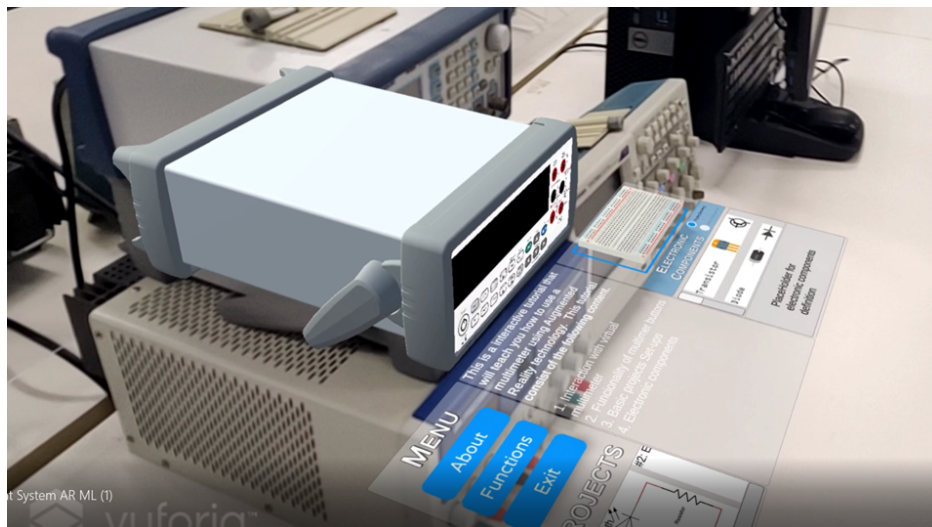


Figure 9: AR training scenario: object tracking and superimposition of a 3D object

488 4. Experimental Results

489 In this section, performance for DL and AR frameworks are discussed.

490 4.1. Object Detection

491 The dataset used in this study is a collection of 643 images with anno-
492 tations. The dataset is divided into four classes: multimeter, oscilloscope,
493 power supply, and wave generator. The collected samples were randomly split
494 into training and test sets with the ratio of 70% and 30%, respectively. We
495 employ commonly used evaluation metrics such as precision, recall, and mAP
496 to evaluate the model performance in the application.

497 4.2. Evaluation Metrics

- 498 • Precision: The percentage of positive detections that were correct is
499 referred to as precision. If a model produces no false positives, it has a
500 precision of 1.0. Equation (2) describes precision as the True Positive
501 divided by the sum of the True Positive (TP) and False Positive (FP).
502 TP is defined as a correct prediction of the positive class, whereas FP
503 is an incorrect prediction of negative class as the positive class.

$$504 \text{ Precision} = \frac{\text{TP}}{\text{TP} + \text{FP}} \quad (2)$$

- 505 • Recall: The percentage of true positives that were correctly identified
506 by the model. A model with a recall of 1.0 produces zero false negatives.
507 Recall can be computed as a ratio of True Positives predictions and the
508 sum of TP and False Negatives (FN), as shown in Equation (3). FN is
509 defined as an incorrect prediction of the positive class as the negative
510 class.

$$511 \text{ Recall} = \frac{\text{TP}}{\text{TP} + \text{FN}} \quad (3)$$

- 512 • Intersection over Union (IoU): It is also known as the Jaccard index
513 used for measuring the similarity and diversity of sample sets. In an
514 object detection task, it describes the similarity between the predicted
515 bounding box and the ground truth bounding box. Equation (4) ex-
516 presses IoU in terms of area of the prediction and ground truth bound-
517 ing boxes.

$$518 \text{ IoU} = \frac{\text{Area of Overlap}}{\text{Area of Union}} \quad (4)$$

519 It is important to define a threshold to define what is the correctness
 520 of the prediction for IoU.

$$\begin{aligned}
 & T \leftarrow \text{Threshold} \\
 & \text{IoU} \geq T \rightarrow \text{Correct} \\
 & \text{IoU} < T \rightarrow \text{Incorrect}
 \end{aligned}
 \tag{5}$$

522 • mean Average Precision (mAP): It takes under consideration both pre-
 523 cision and recall. It is also the area beneath the precision–recall curve.
 524 The mAP can be computed by

$$\text{mAP} = \frac{\sum_{k=1}^n AP_k}{n}
 \tag{6}$$

526 where AP_k is the average precision of class k , and n is the number
 527 of classes.

528 Figure 10 shows our model during inference when the new dataset was fed
 529 to the model. It demonstrates the correct detection of four types of lab equip-
 530 ment in a single shot when the confidence threshold value (i.e., the threshold
 531 related to the confidence score to determine whether the detection is an ob-
 532 ject of interest or not. Confidence scores of the predicted bounding boxes
 533 above the threshold value are considered as positive boxes, or vice versa) is
 534 greater or equal to 90%. The experimental results shown in Table 2 support
 535 that our model has a high mAP. In practice, the DL model can recognize all
 536 of the electrical lab equipment that has been pre-selected.

Table 2: Mean Average Precision with Different IoU score of the Trained MobileNet-SSD V2 model.

Description	IoU	mAP
Average Precision	0.50 : 0.95	0.814
	0.50	0.976
	0.75	0.954

537 Table 2 shows the average precision and average recall for a given IoU
 538 score and mAP. The IoU is a range between 0.50 and 0.95. Using 193 test-
 539 ing images, the average precision of our proposed model achieved a mAP of
 540 81.4% and an average recall of 85.3%. Some failure cases were due to the low

541 ambient lighting and a lack of training datasets with varying lighting condi-
542 tions.

543 The DL model deployed on a mobile device uses CPU resources of the
544 device to infer and predict objects. We ran the DL model on two different
545 mobile devices to evaluate performances of devices for real-time prediction.
546 We used the frame per second (FPS) unit, which measures the number of
547 images that the mobile device screen displays every second.

548 According to Table 3, Samsung has a performance of 8.5 FPS, and One
549 plus has a performance of 5.5 FPS, indicating that the device hardware re-
550 sources are required to accelerate the inference performance.

551 4.3. *Augmented Reality*

552 Detecting a multimeter in real-time is a good way to test the accuracy
553 and precision of AR-based object detection. Figure 11 shows two mobile
554 devices with three different luminous intensities of 25 lux, 150 lux, and 350
555 lux. In addition, we included various distances between the mobile camera
556 and the multimeter in our evaluation to understand how good our scanning
557 process was when collecting data points from the multimeter. This evaluation
558 enables us to determine the optimal room lighting configuration for good AR-
559 based object detection.

560 We included a toggle button in the test AR scenario during the eval-
561 uation to indicate whether the application keeps detecting the multimeter.
562 Table 4 shows the results of the AR-based detection experiments. Due to the
563 camera’s lack of focus, we discovered that our camera was not tracking the
564 multimeter during our preliminary results. We included a script in our Unity
565 engine project that allowed us to focus on the mobile camera. The evaluation
566 table includes focus parameters that will help us decide whether to include
567 this feature in the AR experience. We chose 50 cm and 100 cm for our eval-
568 uation because these are the typical distances between the lab equipment
569 and the students. The final column contains the result in True/False format,
570 indicating whether the multimeter was detected. We concluded that Vuforia
571 can detect objects even in low light conditions. However, the distance will
572 have an impact on the detection results. According to our table evaluation,
573 the focus parameter increases the likelihood of detecting a multimeter in
574 different light intensities, but it also depends on the camera resolution.

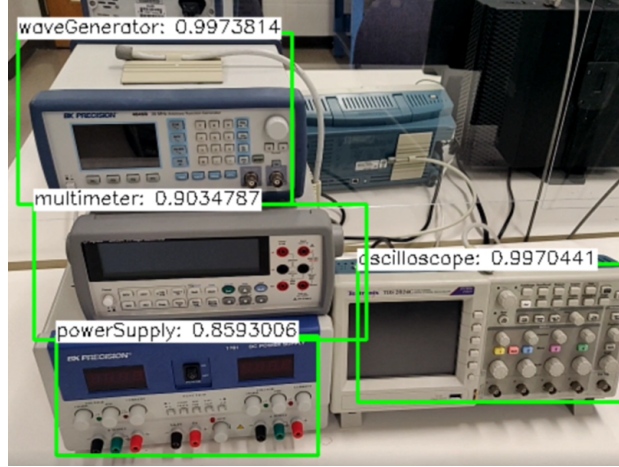


Figure 10: Example of automatic equipment detection by the DL model. The number above each green bounding box indicates confidence score of the model, which is the probability that a bounding box contains an object of interest, for the detection.

Table 3: Mobile Device Hardware Specification and FPS during Inference.

Mobile Device	CPU	RAM	FPS
Samsung S21 Ultra	Samsung Exynos 2100	12 GB	8.5
One Plus 6T	Octa-core Kryo 385	6 GB	5.5



Figure 11: Image reference of Samsung s21 camera with a light intensity of 350 lux (**Left**) and 25 lux (**Right**).

Table 4: AR-based object detection experiments using different devices, luminous intensities, distances between mobile camera and multimeter, and camera’s focus.

Device	luminous inten- sities	Distance (cm)	Focus	Detection Status
1	25	50	No	Yes
1	25	100	No	No
1	25	50	Yes	Yes
1	25	100	Yes	Yes
1	150	50	No	Yes
1	150	100	No	No
1	150	50	Yes	Yes
1	150	100	Yes	Yes
1	350	50	No	Yes
1	350	100	No	Yes
1	350	50	Yes	Yes
1	350	100	Yes	Yes
2	25	50	No	Yes
2	25	100	No	No
2	25	50	Yes	Yes
2	25	100	Yes	No
2	150	50	No	Yes
2	150	100	No	No
2	150	50	Yes	Yes
2	150	100	Yes	No
2	350	50	No	Yes
2	350	100	No	No
2	350	50	Yes	Yes
2	350	100	Yes	Yes

575 5. Conclusions and Future Work

576 In this study, we developed an interactive multimeter tutorial using deep
577 learning and augmented reality. We integrated a deep learning model, namely
578 MobileNet-SSD v2, and an AR target database into a game engine to detect
579 objects automatically. Unity3D was used to create the augmented tutorial,
580 which includes a mobile game infrastructure. The tutorial functions as a
581 virtual manual for the equipment, which provides an immersive experience
582 by projecting holograms on objects recognized by the app via a mobile cam-
583 era. In the future, we will create tutorials for additional lab equipment. One
584 application will be the addition of a 3D interactive breadboard in the app
585 to help students understand electrical circuits. Another potential enhance-
586 ment of the proposed AR- and AI-based education tool would be to support
587 remote learning, in which students can learn lab equipment through the AR
588 streaming on their mobile devices or personal computers.

589 **Author contributions:** J.E.: writing—original draft, methodology, soft-
590 ware, visualization, data curation; S.P.: conceptualization, methodology,
591 writing—reviewing and editing, supervision, funding acquisition; X.Y.: con-
592 ceptualization, methodology, writing—reviewing and editing, supervision,
593 funding acquisition; Q.N.: writing—reviewing and editing, conceptualiza-
594 tion, funding acquisition. All authors have read and agreed to the published
595 version of the manuscript.

596 **Funding:** This research was funded by the National Science Foundation
597 #2129092 and #2129093, 2021.

598 References

- 599 Mejías Borrero, A.; Andújar Márquez, J. A pilot study of the effectiveness
600 of augmented reality to enhance the use of remote labs in electrical engi-
601 neering education. *J. Sci. Educ. Technol.* **2012**, *21*, 540–557.
- 602 Singh, G.; Mantri, A.; Sharma, O.; Dutta, R.; Kaur, R. Evaluating the
603 impact of the augmented reality learning environment on electronics lab-
604 oratory skills of engineering students. *Comput. Appl. Eng. Educ.* **2019**,
605 *27*, 1361–1375.
- 606 Ray, S. A quick review of machine learning algorithms. In Proceedings of
607 the 2019 International Conference on Machine Learning, Big Data, Cloud

608 and Parallel Computing (COMITCon), Faridabad, India, 14–16 February
609 2019; pp. 35–39.

610 Xue, M.; Zhu, C. A study and application on machine learning of artificial
611 intelligence. In Proceedings of the 2009 International Joint Conference on
612 Artificial Intelligence, Hainan, China, 25–26 April 2009; pp. 272–274.

613 Gong, L.; Fast-Berglund, Å.; Johansson, B. A framework for extended reality
614 system development in manufacturing. *IEEE Access* **2021**, *9*, 24796–24813.

615 Nisiotis, L.; Alboul, L. Work-In-Progress-An Intelligent Immersive Learning
616 System Using AI, XR and Robots. In Proceedings of the 2021 7th Inter-
617 national Conference of the Immersive Learning Research Network (iLRN),
618 17 May–10 June 2021; pp. 1–3.

619 Khomh, F.; Adams, B.; Cheng, J.; Fokaefs, M.; Antoniol, G. Software engi-
620 neering for machine-learning applications: The road ahead. *IEEE Softw.*
621 **2018**, *35*, 81–84.

622 Hu, M.; Weng, D.; Chen, F.; Wang, Y. Object Detecting Augmented Reality
623 System. In Proceedings of the 2020 IEEE 20th International Conference
624 on Communication Technology (ICCT), Nanning, China, 28–31 October
625 2020; pp. 1432–1438.

626 Ang, I.J.X.; Lim, K.H. Enhancing STEM education using augmented reality
627 and machine learning. In Proceedings of the 2019 7th International Con-
628 ference on Smart Computing & Communications (ICSCC), Miri, Malaysia,
629 28–30 June 2019; pp. 1–5.

630 Thiwanka, N.; Chamodika, U.; Priyankara, L.; Sumathipala, S.; Weerasuriya,
631 G. Augmented Reality Based Breadboard Circuit Building Guide Applica-
632 tion. In Proceedings of the 2018 3rd International Conference on Informa-
633 tion Technology Research (ICITR), Moratuwa, Sri Lanka, 5–7 December
634 2018; pp. 1–6.

635 Sandoval Pérez, S.; Gonzalez Lopez, J.M.; Villa Barba, M.A.; Jimenez Be-
636 tancourt, R.O.; Molinar Solís, J.E.; Rosas Ornelas, J.L.; Riberth García,
637 G.I.; Rodriguez Haro, F. On the Use of Augmented Reality to Reinforce
638 the Learning of Power Electronics for Beginners. *Electronics* **2022**, *11*, 302.

Technologies, U. Unity Real-Time Development Platform. 2005. Available
online: <https://unity.com/> (accessed on 8 April 2022).

Yu, H.; Chen, C.; Du, X.; Li, Y.; Rashwan, A.; Hou, L.; Jin, P.; Yang, F.;
Liu, F.; Kim, J.; et al. TensorFlow 1 Detection Model Zoo. 2020. Avail-
able online: [https://github.com/tensorflow/models/blob/master/
research/object_detection/g3doc/tf1_detection_zoo.md/](https://github.com/tensorflow/models/blob/master/research/object_detection/g3doc/tf1_detection_zoo.md/) (accessed
on 28 April 2022).

Chen, X.W.; Lin, X. Big data deep learning: Challenges and perspectives.
IEEE Access **2014**, *2*, 514–525.

Alom, M.Z.; Taha, T.M.; Yakopcic, C.; Westberg, S.; Sidike, P.; Nasrin,
M.S.; Hasan, M.; Van Essen, B.C.; Awwal, A.A.; Asari, V.K. A state-
of-the-art survey on deep learning theory and architectures. Electronics
2019, *8*, 292.

Deng, L.; Liu, Y. Deep Learning in Natural Language Processing; Springer,
2018.

Deng, L.; Hinton, G.; Kingsbury, B. New types of deep neural network learn-
ing for speech recognition and related applications: An overview. In Pro-
ceedings of the 2013 IEEE International Conference on Acoustics, Speech
and Signal Processing, Vancouve, BC, Canada, 26–31 May 2013; pp. 8599–
8603.

Nishani, E.; Çiço, B. Computer vision approaches based on deep learning
and neural networks: Deep neural networks for video analysis of human
pose estimation. In Proceedings of the 2017 6th Mediterranean Conference
on Embedded Computing (MECO), Bar, Montenegro, 11–15 June 2017;
pp. 1–4.

LeCun, Y.; Bottou, L.; Bengio, Y.; Haffner, P. Gradient-based learning
applied to document recognition. Proc. IEEE **1998**, *86*, 2278–2324.

Pandiya, M.; Dassani, S.; Mangalraj, P. Analysis of Deep Learning Architec-
tures for Object Detection-A Critical Review. In Proceedings of the 2020
IEEE-HYDCON, Hyderabad, India, 11–12 September 2020; pp. 1–6.

Arora, D.; Garg, M.; Gupta, M. Diving deep in deep convolutional neu-
ral network. In Proceedings of the 2020 2nd International Conference on

671 Advances in Computing, Communication Control and Networking (ICAC-
672 CCN), Greater Noida, India, 18–19 December 2020; pp. 749–751.

673 Girshick, R., Donahue, J., Darrell, T., Malik, J. Region-based convolu-
674 tional networks for accurate object detection and segmentation. IEEE
675 transactions on pattern analysis and machine intelligence **2015**, 38, 142–
676 158.

677 Redmon, J., Divvala, S., Girshick, R., Farhadi, A. You only look once:
678 Unified, real-time object detection. In Proceedings of the IEEE conference
679 on computer vision and pattern recognition, Las Vegas, NV, USA, 27–30
680 June 2016; pp. 779–788.

681 Liu, W.; Anguelov, D.; Erhan, D.; Szegedy, C.; Reed, S.; Fu, C.Y.; Berg,
682 A.C. SSD: Single Shot MultiBox Detector. In Proceedings of the Eu-
683 ropean Conference on Computer Vision, Amsterdam, The Netherlands,
684 11–14 October 2016; pp. 21–37.

685 Ryu, J.; Kim, S. Chinese character detection using modified single shot multi-
686 box detector. In Proceedings of the 2018 18th International Conference on
687 Control, Automation and Systems (ICCAS), PyeongChang, Korea, 17–20
688 October 2018; pp. 1313–1315.

689 Chiu, Y.C.; Tsai, C.Y.; Ruan, M.D.; Shen, G.Y.; Lee, T.T. Mobilenet-
690 SSDv2: An improved object detection model for embedded systems. In
691 Proceedings of the 2020 International conference on system science and
692 engineering (ICSSE), Kagawa, Japan, 31 August–3 September 2020; pp.
693 1–5.

694 Heirman, J.; Selleri, S.; De Vleeschauwer, T.; Hamesse, C.; Bellemans, M.;
695 Schoofs, E.; Haeltermann, R. Exploring the possibilities of Extended Reality
696 in the world of firefighting. In Proceedings of the 2020 IEEE international
697 conference on artificial intelligence and virtual reality (AIVR), Utrecht,
698 The Netherlands, 14–18 December 2020; pp. 266–273.

699 Andrade, T.M.; Smith-Creasey, M.; Roscoe, J.F. Discerning User Activity
700 in Extended Reality Through Side-Channel Accelerometer Observations.
701 In Proceedings of the 2020 IEEE International Conference on Intelligence
702 and Security Informatics (ISI), Arlington, VA, USA, 9–10 November 2020;
703 pp. 1–3.

- 704 Dandachi, G.; Assoum, A.; Elhassan, B.; Dornaika, F. Machine learning
705 schemes in augmented reality for features detection. In Proceedings of the
706 2015 Fifth International Conference on Digital Information and Commu-
707 nication Technology and its Applications (DICTAP), Beirut, Lebanon, 29
708 April–1 May 2015; pp. 101–105.
- 709 Sendari, S.; Anggreani, D.; Jiono, M.; Nurhandayani, A.; Suardi, C.
710 Augmented reality performance in detecting hardware components using
711 marker based tracking method. In Proceedings of the 2020 4th Inter-
712 national Conference on Vocational Education and Training (ICOVET),
713 Malang, Indonesia, 19 September 2020; pp. 1–5.
- 714 Mahurkar, S. Integrating YOLO Object Detection with Augmented Real-
715 ity for iOS Apps. In Proceedings of the 2018 9th IEEE Annual Ubiqui-
716 tous Computing, Electronics & Mobile Communication Conference (UEM-
717 CON), New York, NY, USA, 8–10 November 2018; pp. 585–589.
- 718 El Filali, Y.; Krit, S.D. Augmented reality types and popular use cases. Int.
719 J. Eng. Sci. Math. **2019**, 8, 91–97.
- 720 Poetker, B. What Is Augmented Reality? (+Most Common Types of AR
721 Used Today). 2018. Available online: <https://www.g2.com/articles/augmented-reality> (accessed on 8 April 2022).
- 723 Gao, Y.F.; Wang, H.Y.; Bian, X.N. Marker tracking for video-based aug-
724 mented reality. In Proceedings of the 2016 International Conference on
725 Machine Learning and Cybernetics (ICMLC), Jeju Island, Korea, 10–13
726 July 2016; Volume 2, pp. 928–932.
- 727 Sendari, S.; Firmansah, A.; Aripriharta. Performance analysis of augmented
728 reality based on vuforia using 3d marker detection. In Proceedings of the
729 2020 4th International Conference on Vocational Education and Training
730 (ICOVET), Malang, Indonesia, 19 September 2020; pp. 294–298.
- 731 Vidya, K.; Deryl, R.; Dinesh, K.; Rajabommannan, S.; Sujitha, G. Enhanc-
732 ing hand interaction patterns for virtual objects in mobile augmented re-
733 ality using marker-less tracking. In Proceedings of the 2014 International
734 Conference on Computing for Sustainable Global Development (INDIA-
735 Com), New Delhi, India, 5–7 March 2014; pp. 705–709.

- 736 Beier, D.; Billert, R.; Bruderlin, B.; Stichling, D.; Kleinjohann, B. Marker-
737 less vision based tracking for mobile augmented reality. In Proceedings of
738 the The Second IEEE and ACM International Symposium on Mixed and
739 Augmented Reality, Tokyo, Japan, 7–10 October 2003; pp. 258–259.
- 740 Pooja, J.; Vinay, M.; Pai, V.G.; Anuradha, M. Comparative analysis of
741 marker and marker-less augmented reality in education. In Proceedings
742 of the 2020 IEEE International Conference for Innovation in Technology
743 (INOCON), Bangalore, India, 6–8 November 2020; pp. 1–4.
- 744 Batuwanthudawa, B.; Jayasena, K. Real-Time Location based Augmented
745 Reality Advertising Platform. In Proceedings of the 2020 2nd International
746 Conference on Advancements in Computing (ICAC), Malabe, Sri Lanka,
747 10–11 December 2020; Volume 1, pp. 174–179.
- 748 Unal, M.; Bostanci, E.; Sertalp, E.; Guzel, M.S.; Kanwal, N. Geo-location
749 based augmented reality application for cultural heritage using drones.
750 In Proceedings of the 2018 2nd International Symposium on Multidisci-
751 plinary Studies and Innovative Technologies (ISMSIT), Ankara, Turkey,
752 19–21 October 2018; pp. 1–4.
- 753 Argotti, Y.; Davis, L.; Outters, V.; Rolland, J.P. Dynamic superimposition
754 of synthetic objects on rigid and simple-deformable real objects. Comput.
755 Graph. **2002**, 26, 919–930.
- 756 Ketchell, S.; Chinthammit, W.; Engelke, U. Situated storytelling with SLAM
757 enabled augmented reality. In Proceedings of the The 17th International
758 Conference on Virtual-Reality Continuum and its Applications in Industry,
759 Brisbane, QLD, Australia, 14–16 November 2019; pp. 1–9.
- 760 Knopp, S.; Klimant, P.; Schaffrath, R.; Voigt, E.; Fritzsche, R.; Allmacher, C.
761 Hololens ar-using vuforia-based marker tracking together with text recogni-
762 tion in an assembly scenario. In Proceedings of the 2019 IEEE International
763 Symposium on Mixed and Augmented Reality Adjunct (ISMAR-Adjunct),
764 Beijing, China, 10–18 October 2019; pp. 63–64.
- 765 Soulami, K.B.; Ghribi, E.; Labyed, Y.; Saidi, M.N.; Tamtaoui, A.; Kaabouch,
766 N. Mixed-reality aided system for glioblastoma resection surgery using
767 microsoft HoloLens. In Proceedings of the 2019 IEEE International Con-
768 ference on Electro Information Technology (EIT), Brookings, SD, USA,
769 20–22 May 2019; pp. 79–84.

- 770 Lee, J.D.; Wu, H.K.; Wu, C.T. A projection-based AR system to display
771 brain angiography via stereo vision. In Proceedings of the 2018 IEEE 7th
772 Global Conference on Consumer Electronics (GCCE), Nara, Japan, 9–12
773 October 2018; pp. 130–131.
- 774 Vuforia Developer Library. Introduction to Model Targets. 2021.
775 Available online: [https://library.vuforia.com/articles/Solution/
776 introduction-model-targets-unity.html](https://library.vuforia.com/articles/Solution/introduction-model-targets-unity.html) (accessed on 8 April 2022).
- 777 Zhang, S.; Tian, J.; Zhai, X.; Ji, Z. Detection of Porcine Huddling Behaviour
778 Based on Improved Multi-view SSD. In Proceedings of the 2020 Chinese
779 Automation Congress (CAC), Shanghai, China, 6–8 November 2020; pp.
780 5494–5499.
- 781 Rios, A.C.; dos Reis, D.H.; da Silva, R.M.; Cuadros, M.A.d.S.L.; Gamarra,
782 D.F.T. Comparison of the YOLOv3 and SSD MobileNet v2 Algorithms
783 for Identifying Objects in Images from an Indoor Robotics Dataset. In
784 Proceedings of the 2021 14th IEEE International Conference on Industry
785 Applications (INDUSCON), Sao Paulo, Brazil, 15–18 August 2021; pp.
786 96–101.
- 787 Phadnis, R.; Mishra, J.; Bendale, S. Objects talk-object detection and pat-
788 tern tracking using tensorflow. In Proceedings of the 2018 Second In-
789 ternational Conference on Inventive Communication and Computational
790 Technologies (ICICCT), Coimbatore, India, 20–21 April 2018, pp. 1216–
791 1219.
- 792 Kilic, I.; Aydin, G. Traffic sign detection and recognition using tensorflow’s
793 object detection API with a new benchmark dataset. [-45] In Proceedings
794 of the 2020 International Conference on Electrical Engineering (ICEE),
795 Istanbul, Turkey, 25–27 September 2020; pp. 1–5.
- 796 Lin, T. LabelImg, 2015. <https://github.com/tzutalin/labelImg> (ac-
797 cessed on 8 April 2022)
- 798 Ren, S.; He, K.; Girshick, R.; Sun, J. Faster r-cnn: Towards real-time object
799 detection with region proposal networks. In Proceedings of 28th Annual
800 Conference on Neural Information Processing Systems, Montreal, Canada,
801 7–12 December 2015; pp. 91–99.

- 802 Park, Y.; Chin, S. An Efficient Method of Scanning and Tracking for AR.
803 Int. J. Adv. Cult. Technol. **2019**, 7, 302–307.
- 804 Enoxsoftware. About OpenCV for Unity. 2016. [https://](https://enoxsoftware.com/opencvforunity/documentation/about-opencv-)
805 enoxsoftware.com/opencvforunity/documentation/about-opencv-
806 [for-unity](https://enoxsoftware.com/opencvforunity/documentation/about-opencv-) (accessed on 8 April 2022).